

## Effects of geogrid properties on pullout resistance

J. Izawa, Y. Ishihama & J. Kuwano

*Department of Civil Engineering, Tokyo Institute of Technology, Japan*

A. Takahashi

*Department of International Development Engineering, Tokyo Institute of Technology, Japan*

H. Kimura

*Maeda Corporation, Japan (formerly Tokyo Institute of Technology)*

**ABSTRACT:** Study on the pullout resistance was made on the model geogrids. The first sense, special attention was directed to see the effects of the shape of geogrids. All the model geogrids had the same horizontal surface area, but the dimensions of longitudinal and transverse elements were changed to investigate the effects of two vertical areas, i.e. longitudinal and transverse vertical areas, on the pullout resistance were investigated. It turned out that the geogrids of the same horizontal area, stiffness and thickness had the same friction angle between soil and geogrid, but apparent cohesion, displacement and strain distribution were different. The effects of stiffness of the geogrid were investigated in the second sense. Three model geogrids had the same shape and surface friction, but the stiffness was different. The peak pullout resistance of the stiff geogrid was obtained at the small pullout displacement. Difference in stiffness especially affected at the beginning of the pullout test.

### 1 INTRODUCTION

Various geogrids are widely utilized and contribute the improvement of stability of embankments. It has been recognized that pullout resistance is important when the stability of reinforced embankment is examined. Although material properties as well as pullout resistance of respective geogrids have been investigated, the properties of those geogrids have not been rarely compared each other and little is known about the effects of different material properties on pullout resistance. The material properties and pullout resistances of eleven major geogrids used in Japan were summarized and discussed by Kuwano et al. (1999) based on the data presented in the reports published by Public Works Research Center. It was found from the summarized data of the major geogrids that pullout resistance seems to depend more on the strength of soils than the geogrid properties such as tensile strength, stiffness etc. Strains at pullout failure are smaller for the stiffer grids and for the lower vertical stress. However, as the above-mentioned geogrids were of various types in the materials, shapes and so on, the geogrid properties affecting the pullout resistance were not clearly identified. In this study, model geogrids made of polycarbonate plate were used for pullout tests. Special attention was directed to look at the effects of the shape and the stiffness of geogrids.

### 2 OUTLINE OF PULLOUT TEST

Figure 1 illustrates the pullout test apparatus used in this study. The geogrid was laid in the model ground of 300mm in length, 150mm in width and 178mm in height. It was held by a clamp, which was connected to a jack through a load cell to measure the pullout force. The width of the geogrid was made to be 10mm less than that of the soil container to reduce the effects of the side walls. The vertical stress was applied uniformly by the air pressure in the rubber bag put on the soil. Four wires were attached to the geogrid. They were used to measure the displacements of the respective points of geogrid by LVDTs. Points of measurements in this study are shown in Figure 2.

The model ground of Toyoura sand was made by air pluviation to achieve the relative density of 80%. The area of contact between the geogrid and the soil was kept constant during the pullout test by leaving the 50mm geogrid behind the soil as shown in Figure 4. Pullout tests were made at a rate of 1mm/min under the vertical stress,  $\sigma_v$ , of 15, 25 and 35 kPa. The tests were finished at 45mm because of the limitation in the stroke of the jack.

### 3 EFFECTS OF GEOGRID SHAPE

#### 3.1 Model geogrid

Model geogrids used for pullout tests in this study were made of polycarbonate plate. They were

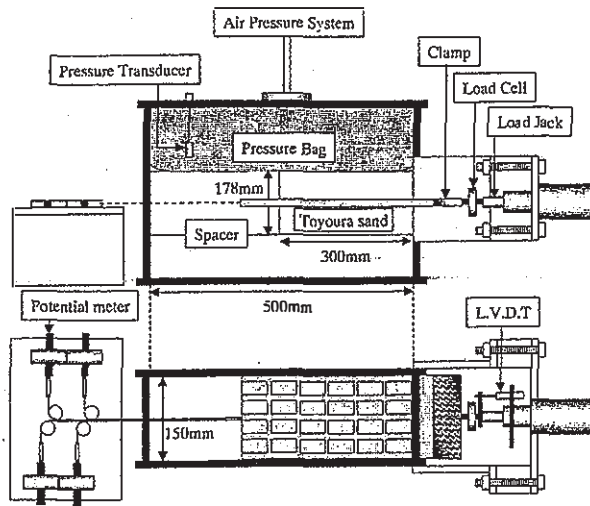


Figure 1. The pullout apparatus.

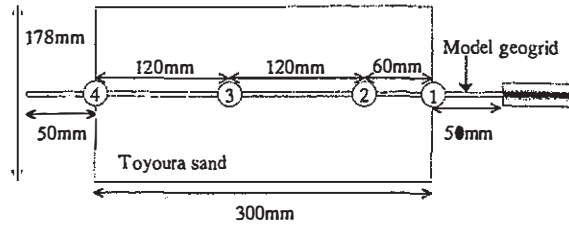


Figure 2. Points of measurement.

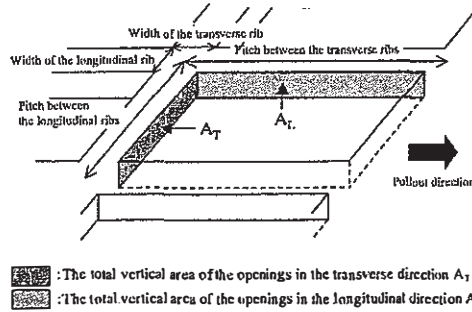


Figure 3. Schematic view of model geogrid.

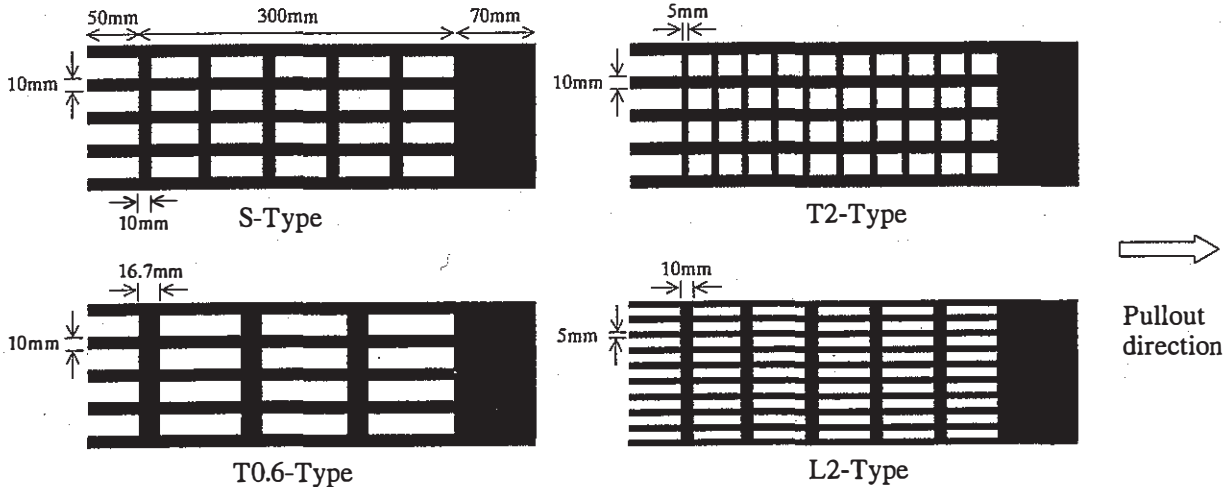


Figure 4. Configurations of model geogrid.

140mm in width and 420mm in length, i.e. as schematically shown in Figure 2, 20mm for clamping, 50mm for the front of a soil specimen, 300mm in the soil and 50mm behind the soil. Five different types of geogrids were prepared to have different opening, rib width and thickness. However, the total horizontal surface area was kept to be same,  $39,000\text{mm}^2$ , for all model geogrids. Shapes of model geogrids are summarized in Table 1. In the table,  $A_T$  denotes the total vertical area of the openings in the transverse direction, and  $A_L$  is that in the longitudinal direction as schematically illustrated in Figure 3.  $A_T$  and  $A_L$  of standard type (S-type) geogrid were  $900\text{mm}^2$  and  $2,600\text{mm}^2$  respectively.  $A_T$  and  $A_L$  of other type geogrids were changed from S-type by changing the number and the width of the ribs as seen in Table 1.

$A_T$  of T2-type geogrid is the double of that of S-type.  $A_T$  of T0.6-type geogrid is 60% of that of S-type.  $A_L$  of L2-type is about the double of S-type. In the case of T2L2-type, shape of the opening is the same as that of S-type, but the thickness is double. Configurations of model geogrids are shown in Figure 4. Tensile tests on respective geogrids were carried out and the results are summarized in Table 2.

### 3.2 Pullout characteristics

All the geogrids were pulled out without rupture in this sense. Therefore, the pullout resistance was calculated from the total contact area between the both sides of geogrid and the soil as shown by the following equation.

Table 1. Properties of model geogrid.

		S	T2	T0.6	L2	T2L2
Thickness	(mm)	1	1	1	1	2
Pitch between transverse ribs	(mm)	60	30	100	60	60
Pitch between longitudinal ribs	(mm)	32.5	32.5	32.5	15	32.5
Width of the longitudinal rib	(mm)	10	10	10	5	10
Width of the transverse rib	(mm)	10	5	16.7	10	10
$A_T$	(mm <sup>2</sup> )	900	1800	540	900	1800
$A_L$	(mm <sup>2</sup> )	2600	2600	2600	5100	5200

Table 2. Results of tensile tests on respective geogrids.

	Tensile strength (kN/m)	Tensile strain at rupture (%)	Tensile stiffness (kN/m)
S	20.22	5.869	449
T2	19.87	5.935	446
T0.6	20.08	5.890	539
L2	21.64	6.146	473
T2L2	34.64	5.916	845

$$\tau = \frac{F}{2BL_G} \quad (1)$$

where  $\tau$  is the pullout resistance,  $F$  is a pullout force,  $B$  is a geogrid width, and  $L_G$  is a length of geogrid in the soil. Figure 5 is the relationship between front displacement and pullout resistance of the model geogrids under  $\sigma_v = 35 \text{ kPa}$ . Although all the geogrids except T2L2 had almost the same total horizontal surface area, tensile strength and stiffness, the ultimate pullout resistance, called as pullout strength, was different. Pullout strength of T2, L2, S, and T0.6-type geogrid was large in that order. It seemed that the increase in the pullout strength was attributed to the increase in the vertical area of transverse element,  $A_T$ , and that of longitudinal element,  $A_L$ . Further discussion on this will be made later. T0.6-type geogrid required larger pullout displacement to mobilize the certain pullout resistance than other geogrids, though its pullout strength was almost the same as that of S-type.

It is concluded that the pullout characteristics depend on the shape of the geogrid even if the surface friction, the tensile strength and the stiffness are the same.

### 3.3 Friction angle between soil and geogrid

Pullout strengths of the respective geogrids are plotted in Figure 6 against the vertical stress. Strength parameters,  $c_p$  and  $\delta_p$ , in the following equation were determined from the approximate straight lines shown in Figure 6.

$$\tau_f = c_p + \sigma_v \tan \delta_p \quad (2)$$

where  $\tau_f$  is the pullout strength,  $c_p$  and  $\delta_p$  are the apparent cohesion and the friction angle between soil and reinforcement respectively.

Table 3.  $\delta_p$  and  $c_p$ .

	$\delta_p$	$c_p$ (kPa)	$\tan \delta_p / \tan \phi$
S	31.2°	3.365	0.673
T2	32.3°	2.764	0.703
T0.6	33.3°	1.093	0.731
L2	31.4°	5.281	0.679
T2L2	37.3°	6.564	0.849

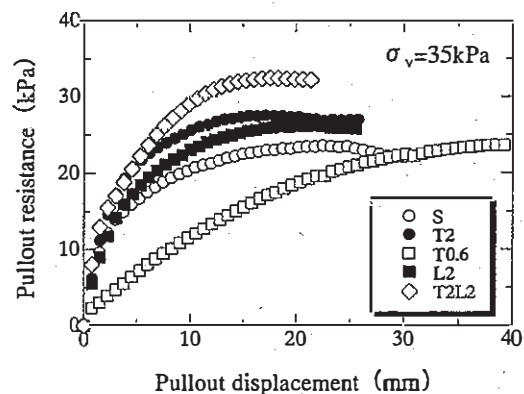


Figure 5. Pullout resistance vs pullout displacement.

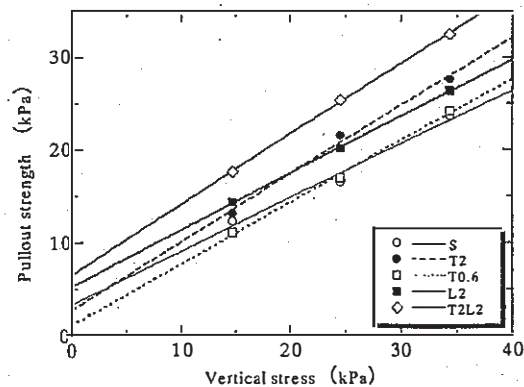


Figure 6. Pullout strength vs vertical stress.

Values of  $c_p$  and  $\delta_p$  together with the friction angle ratio,  $\tan\delta_p/\tan\phi$ , are summarized in Table 3, where  $\phi$  is the internal friction angle of Toyoura sand and  $42^\circ$  for the model ground in this study. It is seen that there is not much difference in the friction angles of the respective geogrids, though the relationship between pullout displacement and pullout resistance heavily depends on the type of geogrid as seen in Figure 5. The difference of  $\delta_p$  among S, T2, T0.6, and L2-type geogrids, is just one to two degrees. Those geogrids have the same total horizontal surface area, tensile strength and stiffness. Therefore, it is thought that the friction angle is not affected much by the shape of geogrid, though the friction on the surface should be the major component of  $\delta_p$ . T2L2-type geogrid, which has a double thickness and high stiffness, showed higher friction angle than other geogrids. Further study is needed on the effects of thickness and stiffness of a geogrid on the pullout resistance.

### 3.4 Deformation of geogrid

Displacements of the respective points of geogrid shown in Figure 2 were measured through the attached wires. Displacements of the respective tests under  $\sigma_v=35\text{kPa}$  are shown in Figures 7 at the pull-out shear stress of  $15\text{kPa}$ . Closer the front, larger the displacements as usually observed. The displacements of T0.6-type geogrid, whose pullout strength was the lowest, were much larger than other geogrids. The displacement was large not only at the front but also at the back. Displacement patterns of S, T2 and L2-type grids were very similar and large in this order. It was the order of small pullout strength. In the case of T2L2-type geogrid, the slope of the displacement distribution is gentler than the other geogrids. It implies that the T2L2 geogrid was pulled out with small tensile strain in it.

Tensile strains were calculated from the displacements at the respective points of the geogrid and shown in Figure 8. They were obtained at a pullout shear stress of  $15\text{kPa}$  under the vertical stress of  $35\text{kPa}$ . Tensile strains in the geogrids are increasing from the back to the front, and therefore tensile stresses. The strains in S, T2 and L2 geogrids are

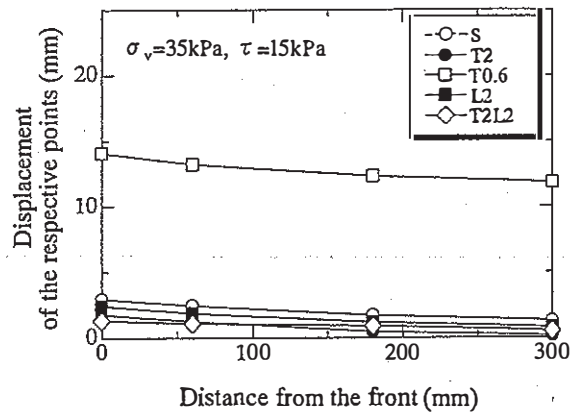


Figure 7. Displacement distribution.

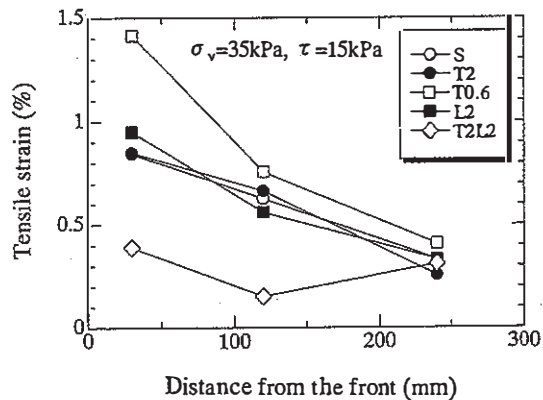


Figure 8. Tensile strain distribution.

almost the same and lower than that in T0.6 geogrid, though the stiffness is the same for these geogrids. Strain in the T2L2 geogrid, which has higher stiffness than the others, is smaller and rather uniform.

## 4 EFFECTS OF GEOGRID STIFFNESS

### 4.1 Model geogrid and outline of Pullout test

Effects of stiffness on pullout resistance were then studied. Three types of model geogrids were prepared. They had same shape, i.e. S-type, and same surface friction, but different tensile stiffness. Poly-

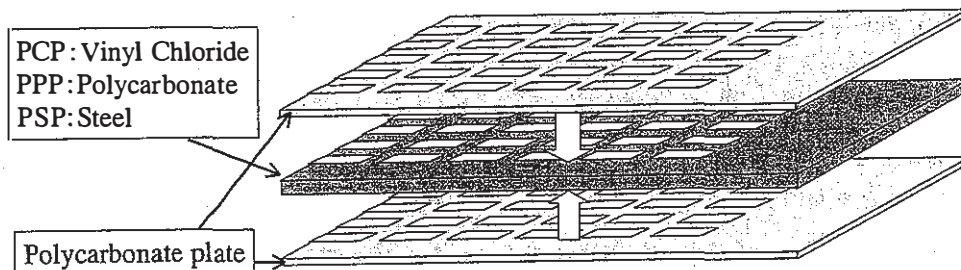


Figure 9. Model geogrid of different stiffness.

carbonate sheets of 0.5mm in thickness were pasted on both sides of 1.0mm thick three different types of sheets, i.e. vinyl chloride, polycarbonate and steel, as shown in Figure 9. The results of tensile test of these geogrids were summarized in Table 4. Pullout tests were conducted with the same procedure as the first test series under the vertical stress of 15, 25, 35 and 50kPa.

#### 4.2 Effects of stiffness on pullout resistance

Figure 10 is the relationship between pullout resistance and pullout displacement under  $\sigma_v=25\text{kPa}$ . The pullout resistance was calculated by equation (1).

Table 4. Properties of model geogrid.

	Intermediate material	Stiffness (kN/m)
PCP	Vinyl Chloride	$5.14 \cdot 10^2$
PPP	Polycarbonate	$1.03 \cdot 10^3$
PSP	Steel	$7.50 \cdot 10^4$

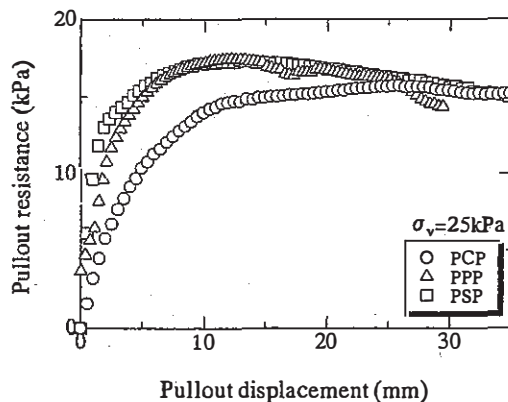


Figure 10. Pullout resistance vs pullout displacement.

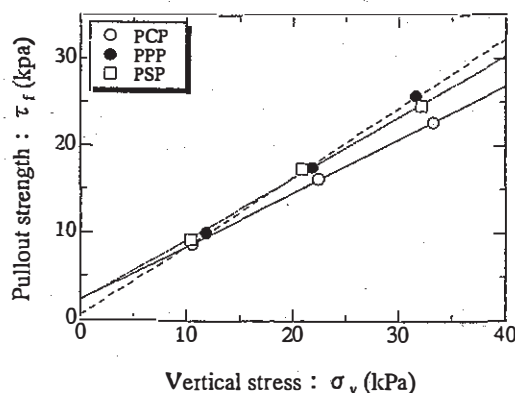


Figure 11. Pullout strength vs vertical stress.

Table 5.  $\delta_p$  and  $c_p$ .

	$\delta_p$	$c_p(\text{kPa})$	$\tan \delta_p / \tan \phi$
PCP	$31.5^\circ$	2.34	0.682
PPP	$38.4^\circ$	0.547	0.881
PSP	$35.0^\circ$	2.26	0.778

PSP, PPP-Type, whose stiffness were (1). PSP, PPP-Type, whose stiffness were higher than PCP-Type, showed the clear peak pullout resistance, and the peak pullout resistances were higher than that of PCP-type. But pullout resistances of the respective geogrids reached almost the same value at the pullout displacement of 25 ~ 30mm. Pullout strengths of the respective geogrids are plotted in Figure 11 against the vertical stress. Values of  $\delta_p$  together with the friction angle ratio,  $\tan \delta_p / \tan \phi$ , are summarized in Table 5. It is seen that there is not much difference in the friction angle of PSP and PCP-Type. And that of PCP-Type is smaller than the other types.

Figure 12 shows pullout resistance under  $\sigma_v=25\text{kPa}$  until the 3mm pullout displacement. In this test series, 50~80% of the peak pullout resistance were obtained at 3mm of pullout displacement. PSP-Type, which has highest stiffness, showed the large pullout resistance at the small pullout displacement. It seems that the effects of stiffness appear also at the small pullout resistance.

Displacements in the geogrids under  $\sigma_v=25\text{kPa}$  are shown in Figure 13 at the pullout resistance of 15kPa. The displacements of PSP-Type geogrid of the highest stiffness were much smaller, and the slope of the displacement distribution is gentler than

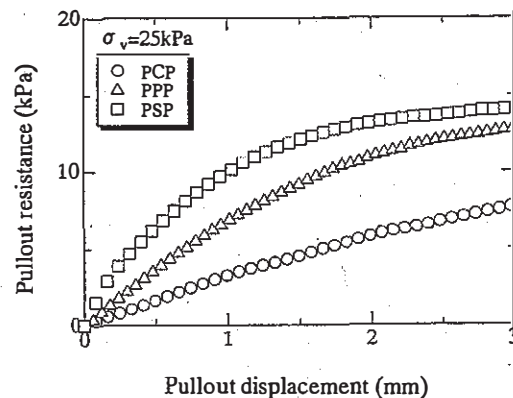


Figure 12. Pullout resistance vs pullout displacement.

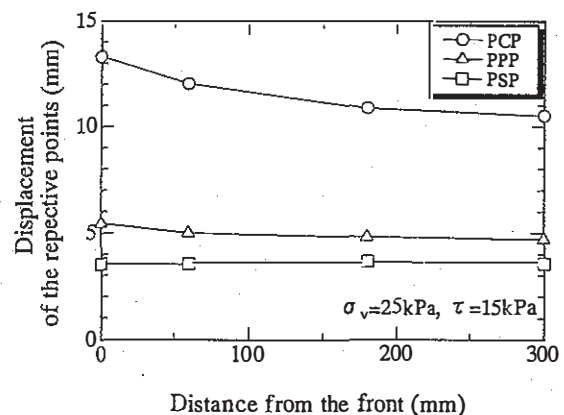


Figure 13. Displacement distribution.

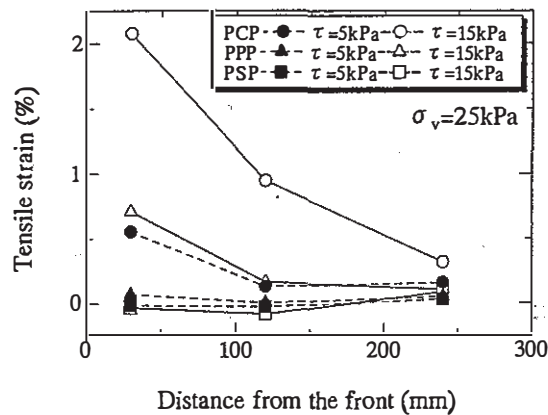


Figure 14. Tensile strain distribution.

the other geogrids. In the case of PCP-Type geogrid, the displacements were larger and the slope of the displacement distribution is steeper than the other geogrids.

Figure 14 show strain distributions at the pullout resistance of 5kPa and 15kPa under  $\sigma_v=25$ kPa. Tensile strains of PSP-Type were almost 0. In the cases of PCP and PPP, tensile strains increased with the increase in the pullout displacement.

## 5 CONCLUSIONS

Study on the pullout resistance was made on the model geogrids. Special attention was directed to see the effects of the shape and stiffness of geogrids. In the first test series, all the model geogrids had the same horizontal surface area, but width of longitudinal and transverse members was changed. In the second test series, all the model geogrid had the

same shape, but materials of geogrid were changed. The followings were obtained in this study.

1. The geogrids of the same horizontal area, stiffness and thickness had the same friction angle between soil and geogrid, but apparent cohesion, displacements and strain distributions in the geogrid were different.
2.  $A_T$ , the total vertical area in the transverse direction, was more effective to increase the pullout resistance than  $A_L$ , the area in the longitudinal direction.
3. Displacements of S, T2 and L2-type geogrids were large in this order. It was the order of small pullout strength. However, the displacement patterns were very similar for the geogrids whose stiffness were the same.
4. The stiff geogrid showed the peak pullout resistance at the small pullout displacement. On the contrary, the soft geogrid needed large pullout displacement and deformation of geogrid to mobilize the peak pullout resistance.
5. Effects of stiffness affected the pullout characteristics especially at the beginning of pullout test.

## REFERENCES

- Kuwano, J., A. Takahashi & H. Kimura 1999. Material properties and pullout characteristics of geogrids used in Japan. *Geosynthetic Engineering Journal*, Vol. 14: 195-204.
- Izawa, J., H. Kimura, J. Kuwano, A. Takahashi, Y. Ishihama 2000. Effects of geogrid shape on pullout resistance. *Geosynthetic Engineering Journal*, Vol. 15: 28-37.
- Japanese Society of Soil Mechanics and Foundation Engineering 1994. Determination of soil/geotextile frictional behavior by direct shear test and/or pull-out test. *Tsuchi-to-Kiso JSSMFE*, Vol. 42, No. 1: 93-102.